Computers and Mathematics with Applications 76 (2018) 831–844

Contents lists available at ScienceDirect

Computers and Mathematics with Applications

journal homepage: www.elsevier.com/locate/camwa

# Localized waves and interaction solutions to a (3+1)-dimensional generalized KP equation

Lili Huang [a,b], Yunfei Yue [a,b], Yong Chen [a,b,c,*]

[a] Shanghai Key Laboratory of Trustworthy Computing, East China Normal University, Shanghai, 200062, China
[b] MOE International Joint Lab of Trustworthy Software, East China Normal University, Shanghai, 200062, China
[c] Department of Physics, Zhejiang Normal University, Jinhua, 321004, China

ARTICLE INFO

*Article history:*
Received 24 December 2017
Received in revised form 6 May 2018
Accepted 20 May 2018
Available online 13 June 2018

*Keywords:*
(3+1)-dimensional generalized KP equation
Hirota bilinear method
Lump
Breather
Rogue wave
Interaction solution

ABSTRACT

Based on the Hirota bilinear method and long wave limit, four kinds of localized waves, namely, solitons, lumps, breathers, and rogue waves are constructed for the (3+1)-dimensional generalized KP equation. N-soliton solutions are obtained by employing bilinear method, then breathers, two breathers and interaction breather solutions are obtained by selecting appropriate parameters on two-soliton solution and four-soliton solution. These breathers own different dynamic behaviors in the different planes. Taking a long wave limit on the two and four soliton solutions under special parameter constraints, one-order lumps and rogue waves, two-order lumps and rogue waves, and interaction solutions between lumps and rogue waves are derived. Applying the same method on the three soliton solution, interaction solutions between kink solitons with periodic solutions, lumps and rogue waves are constructed, respectively. The influence of parameters on the solution is analyzed. The propagation directions, phase shifts, energies and shapes for these solutions can be affected and controlled by the parameters. Moreover, graphics are presented to demonstrate the properties of the explicit analytical localized wave solutions.


## 1. Introduction

The research of nonlinear localized waves is one of the important subjects of contemporary nonlinear mathematical physics. According to the characteristics of the physics and dynamics, nonlinear localized waves are divided into solitons, lumps, breathers and rogue waves, which are key objects in nonlinear physical systems such as nonlinear optics, bio-physics, plasmas, cold atoms, and Bose–Einstein condensates. Solitons own the property of stability and being ionic, while breathers and rogue waves are two kinds of typical localized waves on the background of the plane waves with obvious instability of special nonlinear structure. Theory of solitons [1–3], as one of the three branches of nonlinear science, has become an important research field of nonlinear science and has aroused great interests. Lumps [4–12] are rational function solutions and localized in all directions in the space. Breathers [13–17] are localized breathing waves with a periodic structure in one certain direction and also can be used to elaborate rogue wave phenomena. In accordance with the distribution and propagation direction, breathers can be divided into the Akhmediev breathers [18] and Kuznetsov–Ma breathers [19]. Akhmediev breathers are space-periodic breather solutions, while Kuznetsov–Ma breathers are time-periodic breather solutions. Rogue waves [20–30] are localized in both time and space. The mechanism of rogue waves can be regarded as the high amplitude waves generated by the collision of solitons and breathers. In 1965, the concept of freak rogue wave in

* Corresponding author at: Shanghai Key Laboratory of Trustworthy Computing, East China Normal University, Shanghai, 200062, China.
*E-mail address:* ychen@sei.ecnu.edu.cn (Y. Chen).

https://doi.org/10.1016/j.camwa.2018.05.023
0898-1221/

the ocean was first proposed by Draper [31]. The 'new year's wave' [32], discovered on Jan. 1, 1995 in the North sea, was the most complete recorded rogue wave. In 2007, the optical rogue wave [33] was first spotted by experiments in nonlinear optics. In 2010, the peregrine soliton [34] was observed in nonlinear fiber optics. Up to now, more and more people have paid attention to the study of rogue wave.

In this paper, we study localized waves and interaction solutions for the following $(3+1)$-dimensional generalized KP (GKP) equation [35,36]

$$u_{xxxy} + 3(u_x u_y)_x + u_{tx} + u_{ty} - u_{zz} = 0. \tag{1}$$

If setting $y = x$, Eq. (1) can be reduced to the KP equation [37]; If setting $z = y = x$, Eq. (1) can be reduced to the potential KdV equation [38].

For the GKP equation (1), a lot of literature have studied on it. In [39–44], Wronskian and Grammian solutions, multiple wave solutions, exponential and rational traveling wave solutions, Wronski-type Pfaffian and Gramm-type Pfaffian solutions, lump solutions, the extended system with variable coefficients were studied for the GKP equation, respectively. In [45], multiple-soliton solutions and multiple singular soliton solutions were presented. In [46], a combined Wronskian condition was given to construct Wronskian determinant solutions. In [47], exact periodic kink solitary wave solutions were derived. In [48], breather-type kink soliton, periodic soliton solutions and rogue potential flow for the GKP equation were obtained by utilizing the homoclinic breather limit approach. In [49], Wronskian and linear superposition solutions were derived for a $(3+1)$-dimensional GKP equation with arbitrary real constants. In [50], new exact periodic solitary wave solutions were derived for a new GKP equation with one extra term $u_{tz}$ in multi-temperature electron plasmas. In [51], hyperbolic function solutions, exponential solutions, trigonometric function solutions and rational solutions were obtained. In [52], some exact solutions were derived based on the homoclinic test approach. To our best knowledge, multi-breathers, multi-lumps, multi-rogue waves and interaction solutions to the GKP equation have not been reported yet. It is important to study other rational solutions for the GKP equation (1). Via the method used in [53,54], we will report some new localized wave solutions and interaction solutions for the GKP equation.

Outline of the paper is as follows. In Section 2, $N$-soliton solutions are constructed based on the Hirota bilinear method. In Section 3, via choosing appropriate parameters on the two-soliton solution and four-soliton solution, the breathers, two breathers and interaction between two types of breathers are obtained, their typical dynamical behaviors are shown and analyzed. In Section 4, based on a long wave limit on the multi-soliton solutions, one-order lumps and rogue waves, two-order lumps and rogue waves, and interaction solutions between lumps and rogue waves are proposed and demonstrated. In Section 5, interaction solutions between kink solitons with periodic solutions, lumps and rogue waves are constructed by applying the long wave limits on the three-soliton solution. The Section 6 contains a short summary and further discussion.

## 2. The $N$-soliton solutions

Through applying a dependent variable transformation

$$u = 2(\ln f)_x = 2\frac{f_x}{f}, \tag{2}$$

sends Eq. (1) to the following bilinear form

$$(D_x^3 D_y + D_t D_x + D_t D_y - D_z^2)(f \cdot f) = 0, \tag{3}$$

where $f = f(x, y, z, t)$, all the derivatives $D_x^3 D_y$, $D_t D_x$, $D_t D_y$, and $D_z^2$ are bilinear derivative operators [55] with

$$D_x^\alpha D_y^\beta D_z^\gamma D_t^\delta (f \cdot g) = \left(\frac{\partial}{\partial x} - \frac{\partial}{\partial x'}\right)^\alpha \left(\frac{\partial}{\partial y} - \frac{\partial}{\partial y'}\right)^\beta \left(\frac{\partial}{\partial z} - \frac{\partial}{\partial z'}\right)^\gamma \left(\frac{\partial}{\partial t} - \frac{\partial}{\partial t'}\right)^\delta f(x, y, z, t) g(x', y', z', t')|_{x'=x, y'=y, z'=z, t'=t}. \tag{4}$$

It is apparent that if $f$ solves Eq. (3), then $u = u(x, y, z, t)$ is the solution of Eq. (1) by the transformation (2).

Based on the Hirota bilinear method, the GKP equation (1) has the $N$-order soliton solution (2), with $f$ expressed as the following form,

$$f = \sum_{\mu=0,1} \exp\Big(\sum_{i=1}^{N} \mu_i \eta_i + \sum_{1 \le i < j}^{N} \mu_i \mu_j \ln(A_{ij})\Big), \tag{5}$$

where

$$\begin{gathered} \omega_i = -\frac{k_i^2 p_i - q_i^2}{p_i + 1}, \\ \eta_i = k_i(x + p_i y + q_i z + \omega_i t) + \eta_i^0, \\ A_{ij} = \frac{(p_j+1)(3p_i^2 + 2p_i + p_j)k_i^2 - 3(p_j+1)(p_i+1)(p_i+p_j)k_i k_j + (p_i+1)(3p_j^2 + p_i + 2p_j)k_j^2 + (p_i q_j - p_j q_i - q_i + q_j)^2}{(p_j+1)(3p_i^2 + 2p_i + p_j)k_i^2 + 3(p_j+1)(p_i+1)(p_i+p_j)k_i k_j + (p_i+1)(3p_j^2 + p_i + 2p_j)k_j^2 + (p_i q_j - p_j q_i - q_i + q_j)^2} \\ (i, j = 1, 2, \ldots, N). \end{gathered} \tag{6}$$

with $k_i$, $p_i$, $q_i$ and $\eta_i^0$ arbitrary constants and $\sum_{\mu=0,1}$ the summation total of taking over all possible combinations of $\eta_i, \eta_j = 0, 1 (i, j = 1, 2, \ldots, N)$. Then the $N$-soliton solution can be constructed by substituting (5) with (6) into Eq. (2).

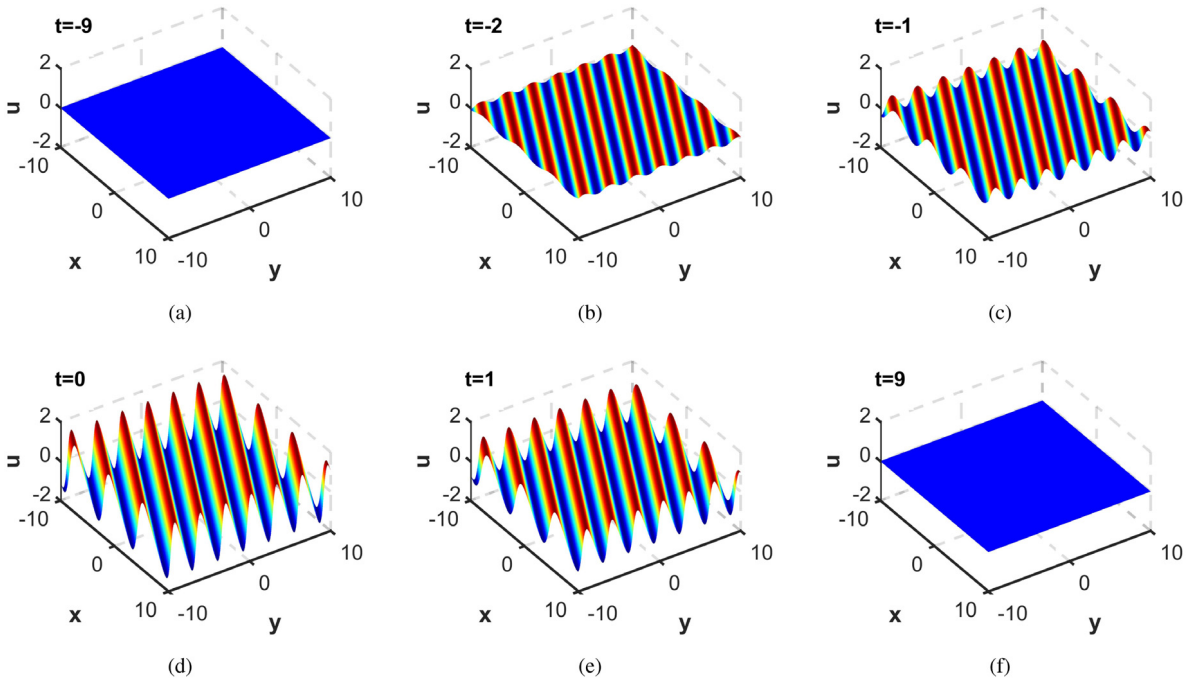


**Fig. 1.** The time evolutions of line breathers for Eq. (1) in the $(x, y)$ plane with parameters given in Eq. (8) at $z = 0$.

## 3. The breather solutions

On the basis of the methods used in the previous works for obtaining breathers, analytical expressions for the breather solutions can be derived by virtue of selecting appropriate parameters for the two-soliton solution in Eq. (2).

Hence, setting $N = 2$ in Eq. (5), then substituting $f$ into the solution (2) of Eq. (1), line breathers can be derived in the $(x, y)$ plane with the parameters in Eq. (2) meeting the following requirements

$$k_1 = k_2^* = aI, \quad p_1 = p_2 = b, \quad q_1 = q_2^* = c + dI. \tag{7}$$

Without loss of generality, setting parameters in the following form

$$a = c = 1, \quad b = d = 2, \quad \eta_1^0 = \eta_2^0 = 0, \tag{8}$$

the function $f$ in Eq. (2) can be restated as

$$\begin{aligned} f \ = \ & 1 + 2\cosh(2z + \frac{4t}{3})\cosh(\frac{t}{3} - z - x - 2y) - 2\sinh(2z + \frac{4t}{3})\cosh(\frac{t}{3} - z - x - 2y) \\ & + \frac{5}{2}\cosh(4z + \frac{8t}{3}) - \frac{5}{2}\sinh(4z + \frac{8t}{3}). \end{aligned} \tag{9}$$

In Fig. 1, global dynamic behaviors with the development of time are demonstrated in the $(x, y)$ plane for the corresponding solution $u$. Here, these periodic line waves are referred to line breathers, and the fundamental line rogue waves can be regarded as the limiting cases of these period line waves. Over time, the periodic line breathers apparently begin at a constant state and achieve the maximum amplitude 1.3926 at $t = 0$, then gradually start damping and go back to the initial constant state in the last. While the line breathers remain parallel and independent of each other during the propagation, their behaviors are changed consisting with the development of time. General breather also can be obtained, which is shown in Fig. 2. Without loss of generality, these breathers present different behavior characteristics with the above same parameters in different planes. In the $(x, t)$ plane, the breather is localized in the $t$ direction, and periodic in the $x$ direction. In the $(y, t)$ plane, it is localized in the $t$ direction, and periodic in the $y$ direction. In the $(z, t)$ plane, it is periodic in the angular bisector of the $z$ axis and $t$ axis. What is more, it is obvious to see that they own different periods.

Using the same method on the four soliton solution (i.e. $N = 4$ in Eq. (5)), setting

$$\begin{aligned} & k_1 = k_2^* = I, \quad k_3 = k_4^* = 2I, \quad q_1 = q_2^* = 1 + I, \quad q_3 = q_4^* = 1 + I, \quad p_1 = p_2 = 1, \\ & p_3 = p_4 = 2 \quad \eta_i^0 = 0 \quad (i = 1, 2, 3, 4), \end{aligned} \tag{10}$$

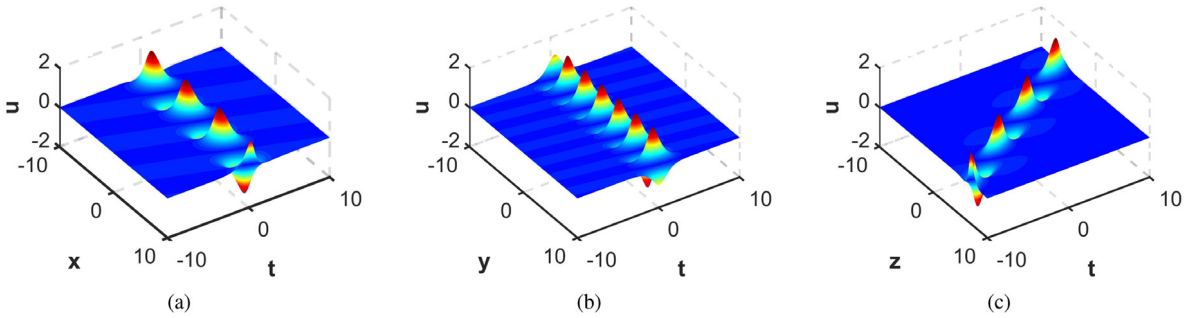


**Fig. 2.** Breathers of Eq. (1) in the $(x, t)$, $(y, t)$ and $(z, t)$ three different planes with the same parameters given in Eq. (8).

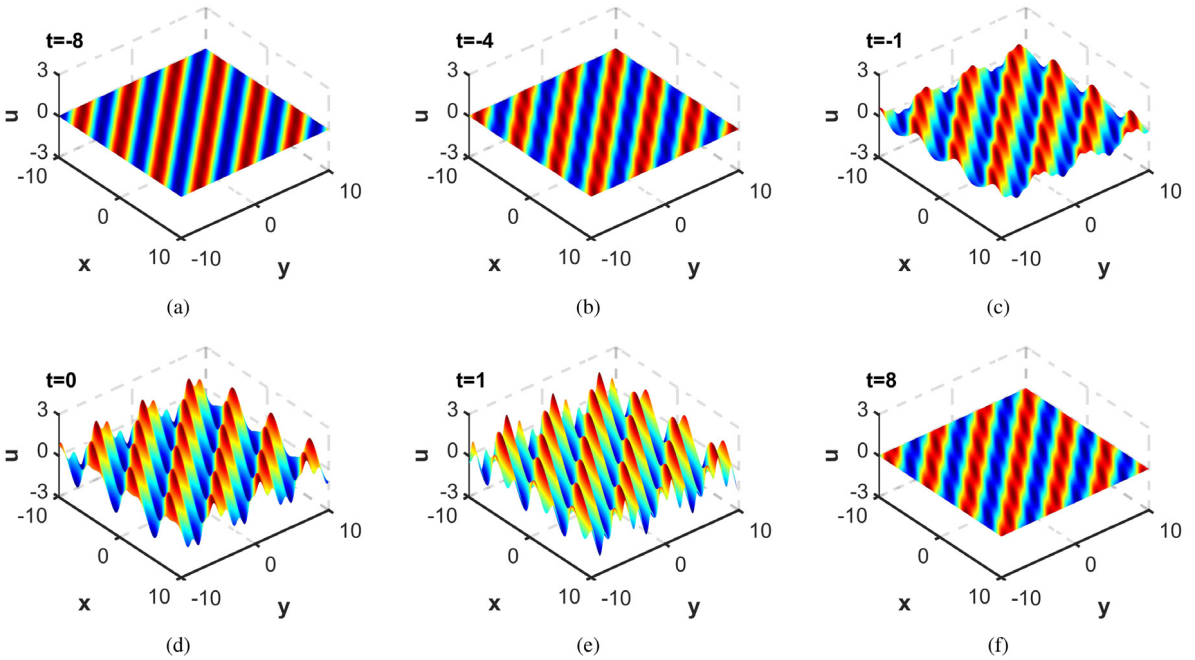


**Fig. 3.** The two line breathers of Eq. (1) in different planes for parameters given in Eq. (10).

two types of interaction solutions between two breathers are available. The process of their collisions is shown in Figs. 3 and 4. Interestingly, the two line breathers are initially separated. As time changed, they are overlapped at $t = 0$, whose amplitude reaches maximum value 1.3743, and eventually spreads separately in Fig. 3. For the general breathers, they are overlapped completely at $t = 0$, whose amplitude reaches maximum value 1.6956 in Fig. 4. Comparing the changes of the amplitude with the two breathes, their values of amplitude fluctuate during the collision, then their values return to initial constant. It is obvious that the collision between two general breathers is elastic.

Similar with the above parameter conditions, interaction solutions between two types breathers can be obtained in $(x, y)$ and $(x, z)$ planes by choosing different parameters. Intersecting general breathers are also can be derived in $(y, z)$ plane. Without loss of generality, setting

$$k_1 = k_2^* = I, \quad k_3 = k_4^* = 2I, \quad p_1 = p_2^* = 1 + I, \quad q_3 = q_4^* = 2 + 2I, \quad q_1 = q_2 = 3, \quad p_3 = p_4 = 2. \tag{11}$$

It is visually shown that their amplitudes change over time, and finally the line breather returns to the initial constant plane, whose dynamic characteristics are presented in Figs. 5 and 6. In $(y, z)$ plane, interaction solution of two general breathers generates a highest amplitude value at the cross point, which is demonstrated in Fig. 7. For $t = -4$, the highest amplitude is $-2.8127$ and the corresponding coordinate is $(-5.8, 5.6)$ in Fig. 7a; for $t = 0$, it is $-2.9417$ at $(0.7, 0.2)$ in Fig. 7b; for $t = 4$, it is 2.0524 at $(8.5, -5)$ in Fig. 7c.

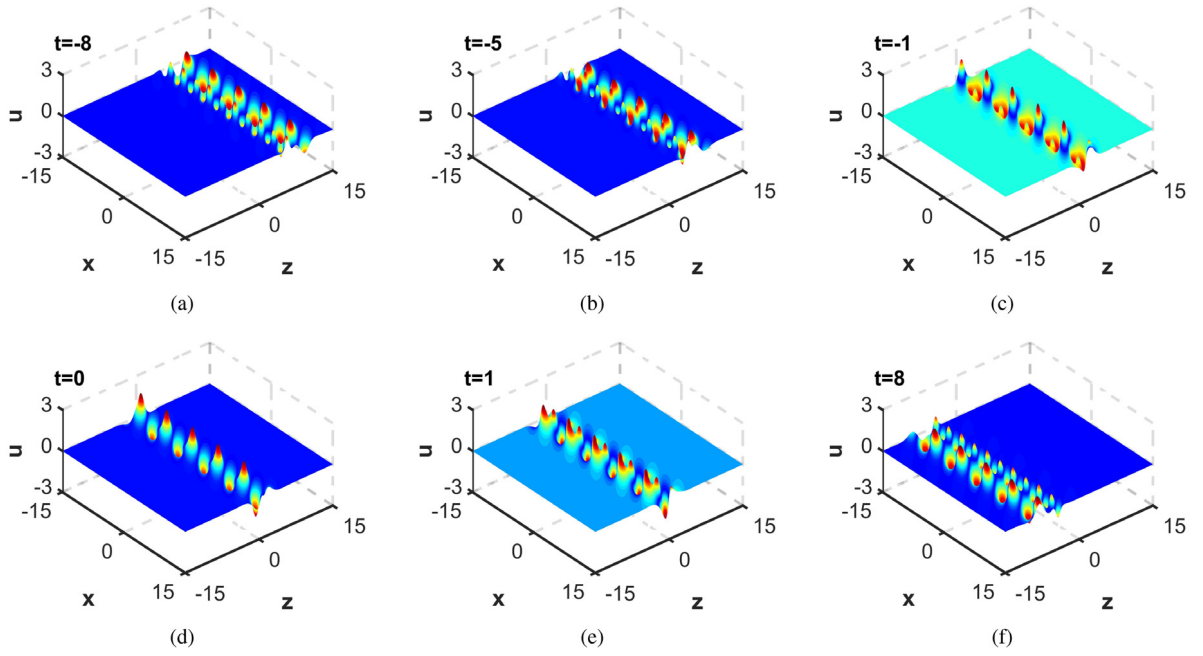


**Fig. 4.** The interaction of two general breathers of Eq. (1) in $(x, z)$ plane for parameters given in Eq. (10).

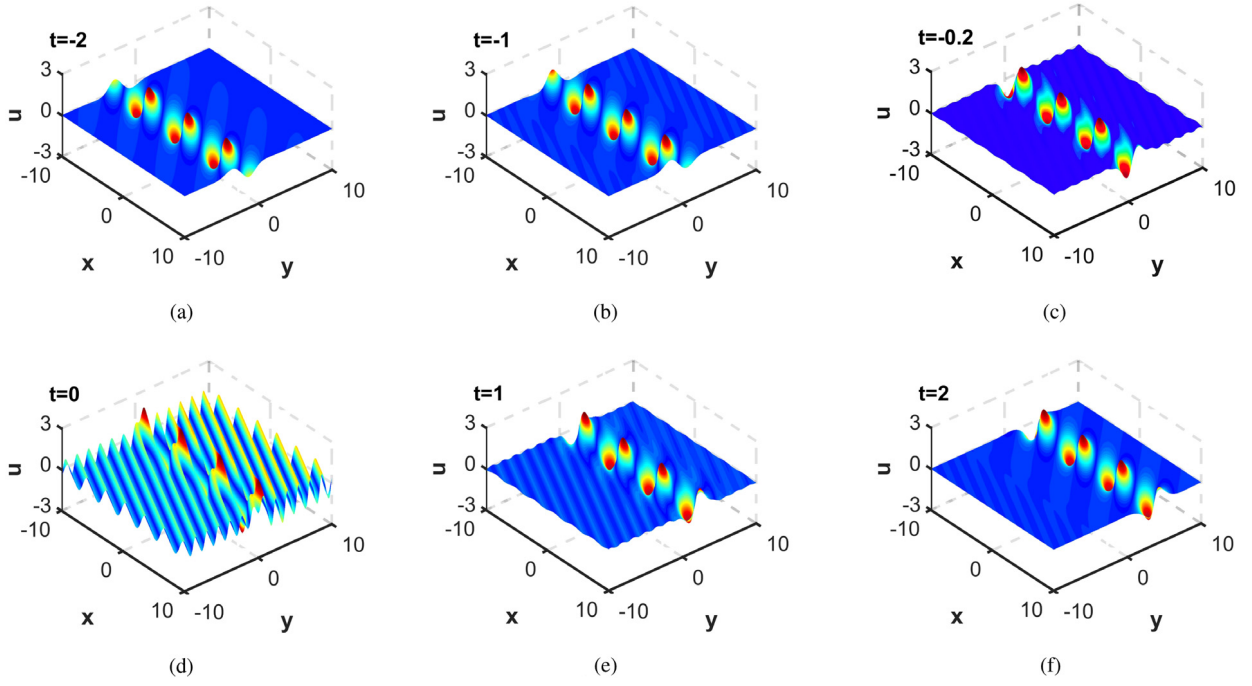


**Fig. 5.** The interaction of two types breathers of Eq. (1) in $(x, y)$ plane for parameters given in Eq. (11) at $z = 0$.

## 4. The lump solution and rogue wave solution

Based on the long wave limits [56,57] on the multi-soliton solutions, we obtained the one-order lumps and rogue waves, two-order lumps and rogue waves, and interaction solutions between lumps and rogue waves, respectively.

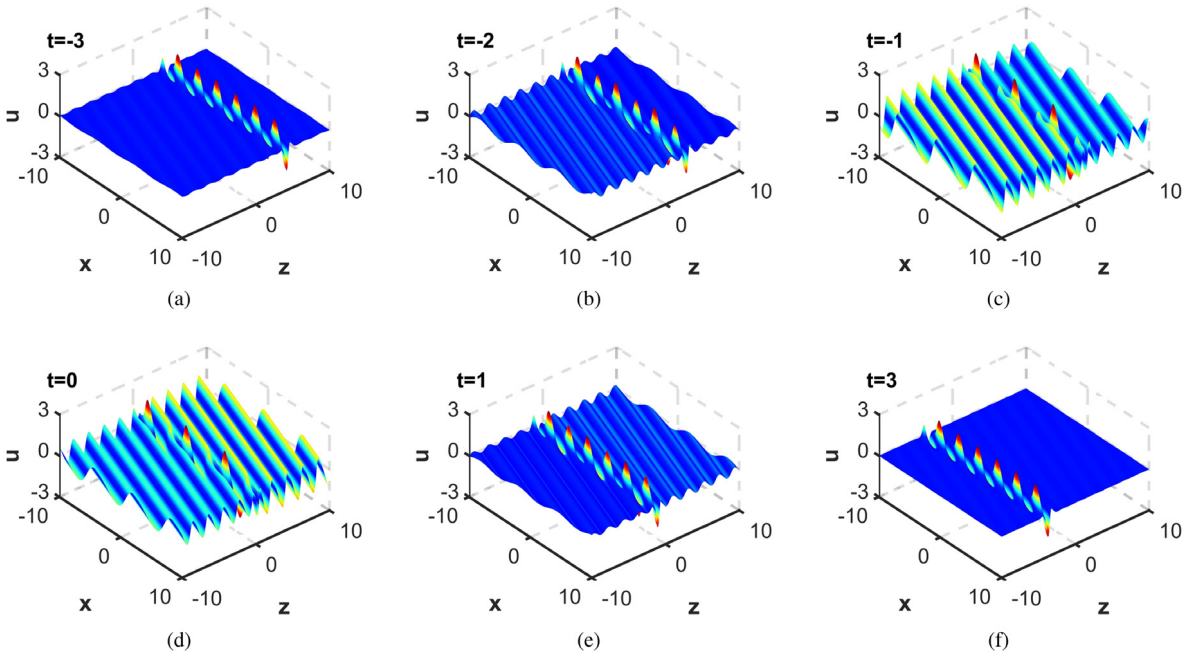


**Fig. 6.** The interaction of two types breathers of Eq. (1) in $(x, z)$ plane for parameters given in Eq. (11) at $y = 0$.

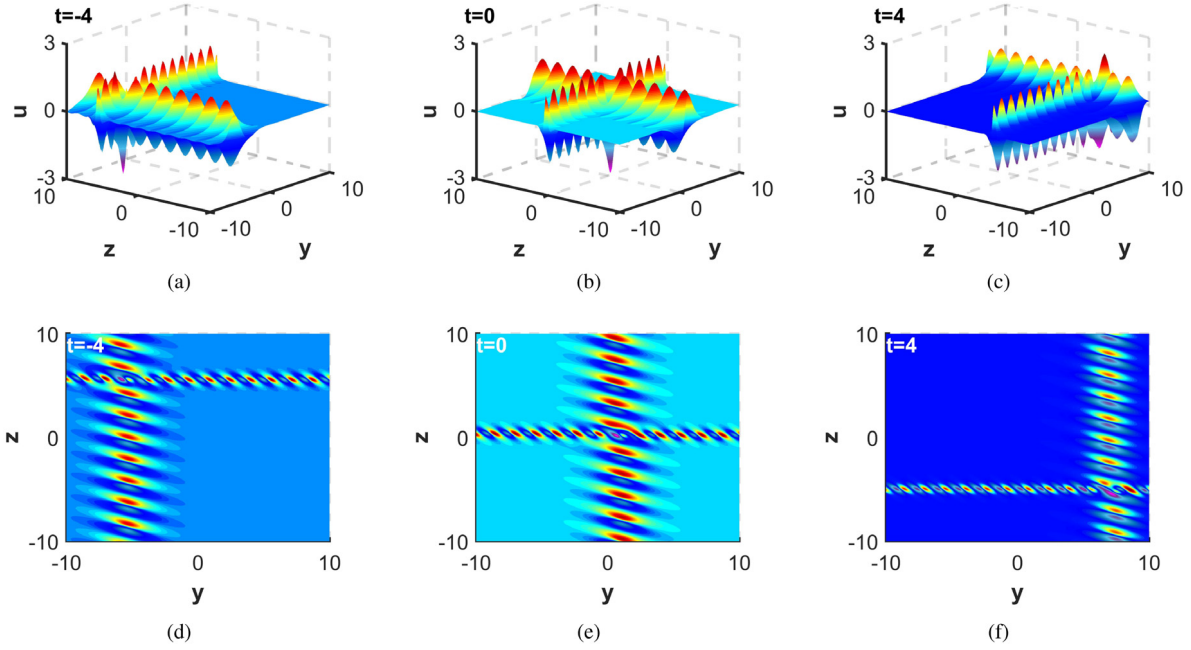


**Fig. 7.** The interaction of two general breathers of Eq. (1) in $(y, z)$ plane for the parameters given in Eq. (11) at $x = 0$. (d), (e) and (f) are density plots of (a), (b) and (c), respectively.

### Case 1. Lump solution

Applying the long wave limits on the two soliton solutions, the rational solution can be obtained. So setting parameters

$$N = 2, \quad k_1 = l_1\epsilon, \quad k_2 = l_2\epsilon, \quad \eta_1^0 = \eta_2^{0*} = I\pi, \tag{12}$$

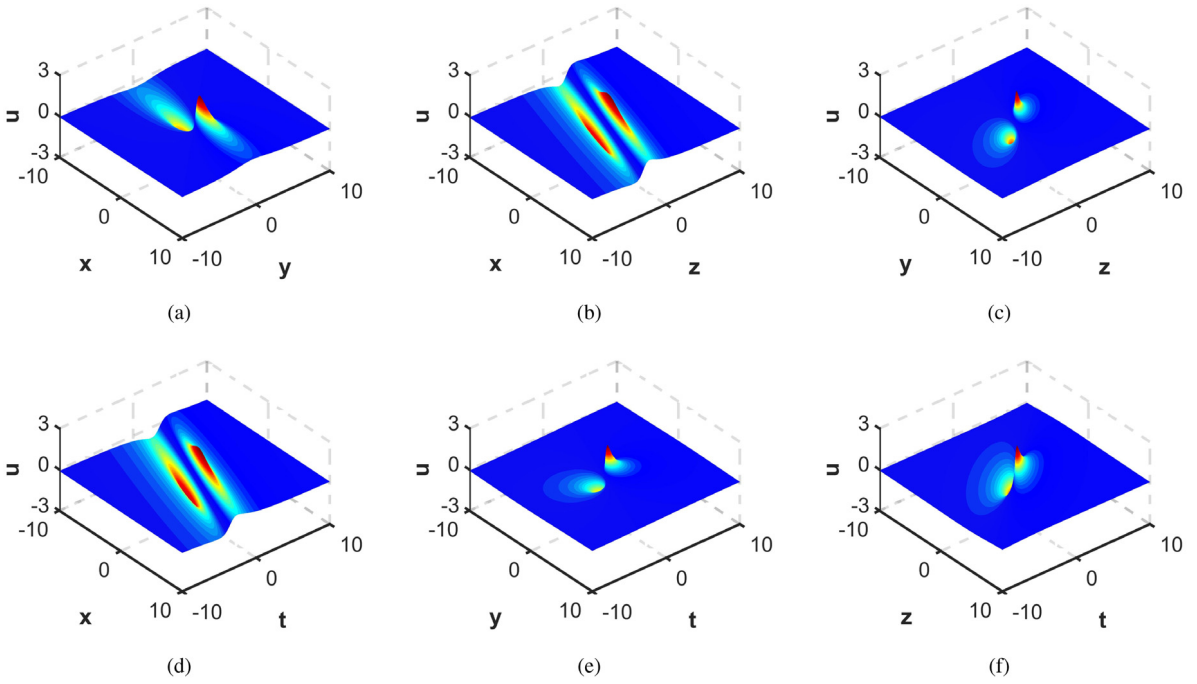


**Fig. 8.** The lump solutions for Eq. (1) in different planes with the parameters $a_1 = 1,\ \ b_1 = 3,\ \ a_2 = 3$, and $b_2 = 1$ in Eq. (13).

and taking the limit as $\epsilon \to 0$ in Eq. (5). The rational solutions of the GKP equation (1) can be derived, which can be written as

$$u = \frac{2(\theta_1 + \theta_2)}{\theta_1\theta_2 + \theta_0}, \tag{13}$$

with

$$\begin{aligned} \theta_0 &= -\frac{6(p_2+1)(p_1+1)(p1+p2)}{((p_1+1)q_2 - q_1(p_2+1))^2}, \\ \theta_i &= x + p_i y + q_i z + \frac{qi^2 t}{p_i + 1} \quad (i = 1, 2). \end{aligned} \tag{14}$$

Setting $p_2 = p_1^*,\ \ q_2 = q_1^*$, it is apparent that the solution $u$ in Eq. (13) is nonsingular. Moreover, this solution shows two kinds of dynamic characteristics. Without loss of generality, assuming $p_1 = a_1 + Ib_1,\ \ q_1 = a_2 + Ib_2$, and $a_1, a_2, b_1, b_2$ are all real constants.

When $a_1 \neq 0$, the trajectory defined along $[x(t), y(t)]$, with

$$\begin{aligned} x + a_1 y + a_2 z + \frac{a_1 a_2^2 - a_1 b_2^2 + 2a_2 b_1 b_2 + a_2^2 - b_2^2}{a_1^2 + b_1^2 + 2a_1 + 1} t - \frac{\sqrt{3a_1(a_1^2 + b_1^2 + 2a_1 + 1)}}{a_1 b_2 - a_2 b_1 + b_2} = 0, \\ b_1 y + b_2 z + \frac{2a_1 a_2 b_2 - a_2^2 b_1 + b_1 b_2^2 + 2a_2 b_2}{a_1^2 + b_1^2 + 2a_1 + 1} t = 0, \end{aligned} \tag{15}$$

the solution $u$ in Eq. (13) can be constant. It is not difficult to find that these rational solutions have been moving in the permanent lumps on the backgrounds of kink states. Lump solutions can be obtained simply by selecting the appropriate parameters and are localized in all directions in the space, which are visually shown in Fig. 8.

If applying the same method to the four soliton solutions, and setting

$$k_1 = l_1\epsilon,\ \ k_2 = l_2\epsilon,\ \ k_3 = l_3\epsilon,\ \ k_4 = l_4\epsilon,\ \ \eta_1^0 = \eta_2^{0*} = \eta_3^0 = \eta_4^{0*} = I\pi, \tag{16}$$

then the corresponding function $f$ has the form given below

$$\begin{aligned} f = &(\theta_1\theta_2\theta_3\theta_4 + a_{12}\theta_3\theta_4 + a_{13}\theta_2\theta_4 + a_{14}\theta_2\theta_3 + a_{23}\theta_1\theta_4 + a_{24}\theta_1\theta_3 + a_{34}\theta_1\theta_2 + a_{12}a_{34} + a_{13}a_{24} + a_{14}a_{23}) \\ &\times l_1 l_2 l_3 l_4 \epsilon^4 + O(\epsilon^5), \end{aligned} \tag{17}$$

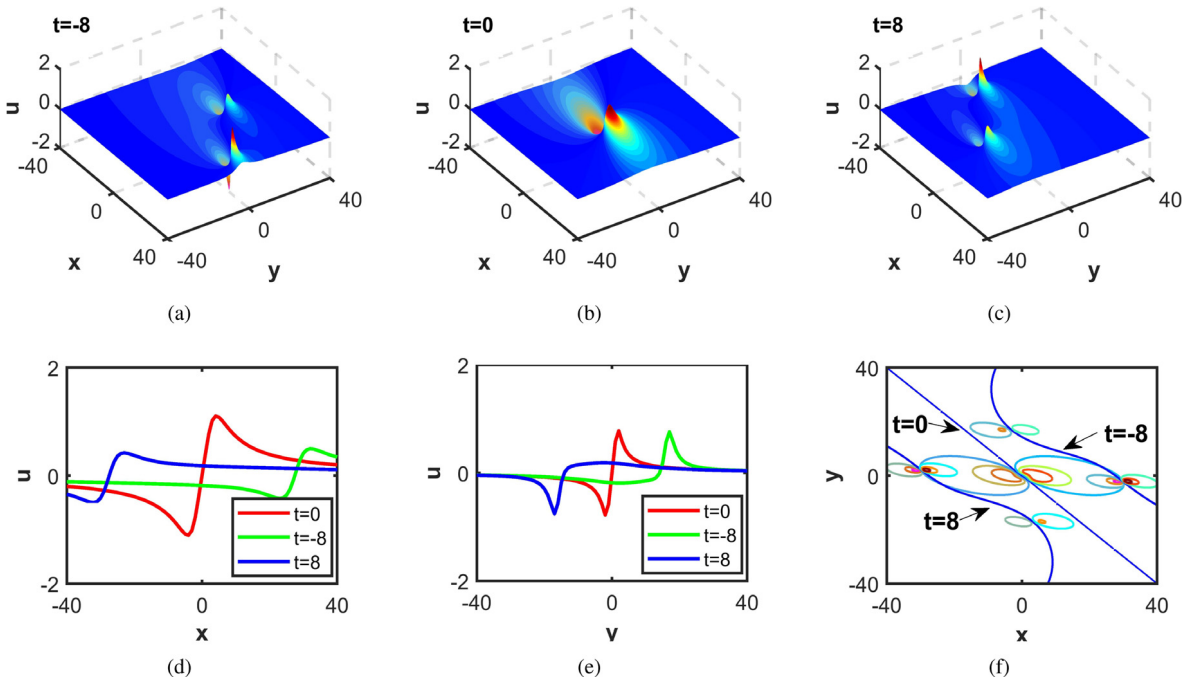


**Fig. 9.** Interaction of the two lump solutions overtaking collision of Eq. (1) in the $(x, y)$ plane for parameters $a_1 = 1,\ b_1 = 2,\ a_2 = 1,\ b_2 = 2,\ c_1 = 2,\ d_1 = 3,\ c_2 = 3,\ d_3 = 1$. (a), (b) and (c) the three-dimensional plots at $t = -8, t = 0, t = 8$, respectively; (d) two-dimensional plot at $y = 0$; (e) two-dimensional plot at $x = 0$; (f) the interaction process.

where

$$\begin{aligned} \theta_i &= x + p_i y + q_i z + \frac{q_i^2}{p_i + 1} t, \\ a_{ij} &= -\frac{6(p_i + 1)(p_j + 1)(p_i + p_j)}{((p_i + 1)q_j - q_i(p_j + 1))^2} \ (i, j = 1, 2, 3, 4). \end{aligned} \tag{18}$$

Similarly, assuming $p_1 = p_2^* = a_1 + b_1 I, p_3 = p_4^* = a_2 + b_2 I, q_1 = q_2^* = c_1 + d_1 I, q_3 = q_4^* = c_2 + d_2 I$, and $a_i, b_i, c_i, d_i, (i = 1, 2)$ are all real constants. When choosing different parameters, different interaction solutions can be obtained. Without loss of generality, setting $a_1 = 1,\ b_1 = 2,\ a_2 = 1,\ b_2 = 2,\ c_1 = 2,\ d_1 = 3,\ c_2 = 3,\ d_3 = 1$, we can obtain two-order lump solution in the $(x, y)$ plane. Its dynamic characteristics are visually shown in Fig. 9. Obviously, the collisions are elastic and the propagation situations can be seen via Fig. 9. The amplitude of the interaction solution reaches 1.1140 at $t = 0$.

**Case 2. Rogue wave solution**

For $N = 2$, when $b_1 = 0$, namely $p_1$ and $p_2$ are all real constants, then line rogue wave can be obtained. This solution is a rational growing and decaying mode. For instance, when $a_1 = 1,\ b_1 = 0,\ a_2 = 2,\ b_2 = 2$, the amplitude changes along the time in the $(x, y)$ plane, and reaches a highest amplitude 2.3077 at $t = 0$, then disappears in the infinity, whose dynamic behaviors are demonstrated in Fig. 10.

For $N = 4$, when $a_1 = 1,\ b_1 = 2,\ a_2 = 1,\ b_2 = 2,\ c_1 = 3,\ c_2 = -2,\ d_1 = d_2 = 0$, appears the interaction solution between two line rogue waves, whose dynamic features are demonstrated in Fig. 11. Similar with single line rogue waves, two line rogue waves arise from the constant background and disappear into the constant background again, whose amplitude reaches a maximum value 3.7635 at $t = 0$ in Fig. 11c. Depending on the special values of the time coordinate $t$, the line rogue wave can be either bright wave or dark one. It should be pointed out that the two interaction line rogue waves are bright rogue wave and dark rogue wave in Fig. 11.

**Case 3. Interaction solutions between lumps and rogue waves**

Based on the parameter selection method of case 1 and case 2, the interaction solutions between lumps and line rogue waves can be presented. Without loss of generality, setting $a_1 = 0.5,\ b_1 = 1,\ a_2 = 0.5,\ b_2 = 1,\ c_1 = -1,\ d_1 = 1,\ c_2 = 3,\ d_2 = 0$, their collision process is shown in the $(x, z)$ plane, which is displayed in Fig. 12. Firstly, a lump moves on the constant background. At the intermediate time, a line rogue wave arises and then interacts with the lump. It is pointed out that the amplitude of lump is significantly increased, when there is complete collision at $t = 0$. Interestingly, the interaction of these two types of localized waves implies a downward deformation of the line rogue wave at $t = 0$. Finally, the line rogue waves disappear into the constant background, and the moving lump is preserved eventually.

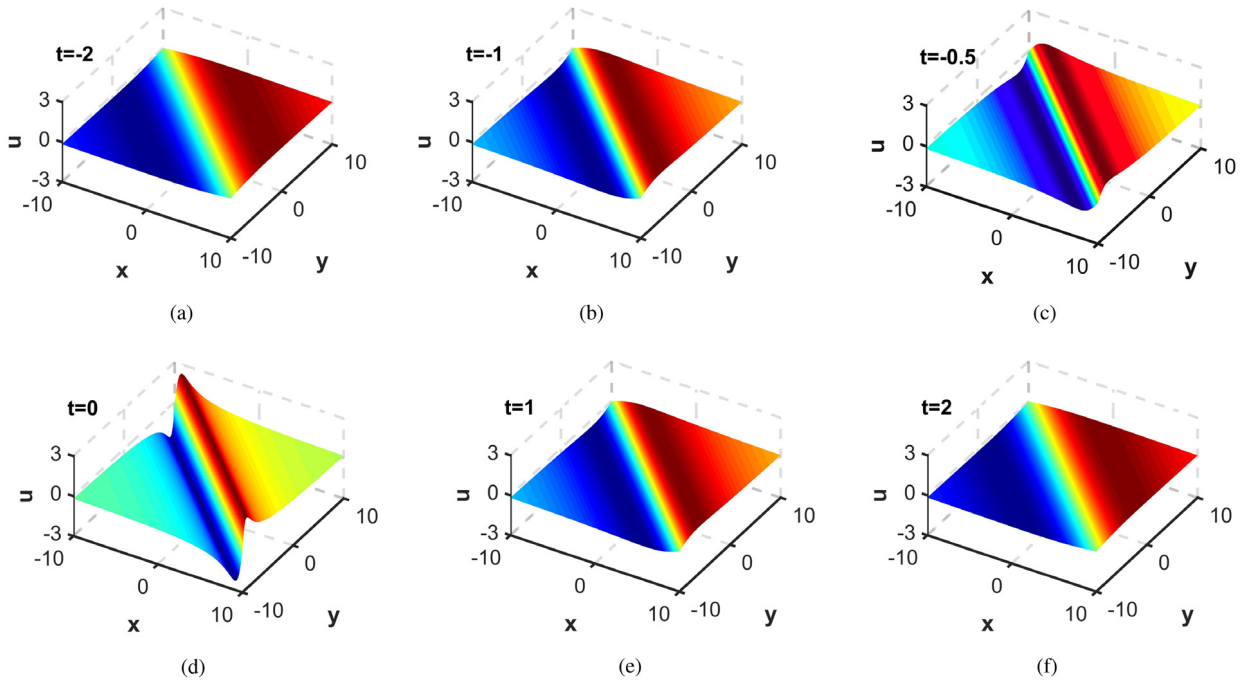


**Fig. 10.** The time evolution of line rogue waves (13) of Eq. (1) in the $(x, y)$ plane for parameters $a_1 = 1,\ \ a_2 = 2,\ \ b_1 = 0,\ \ b_2 = 2$ at $z = 0$.

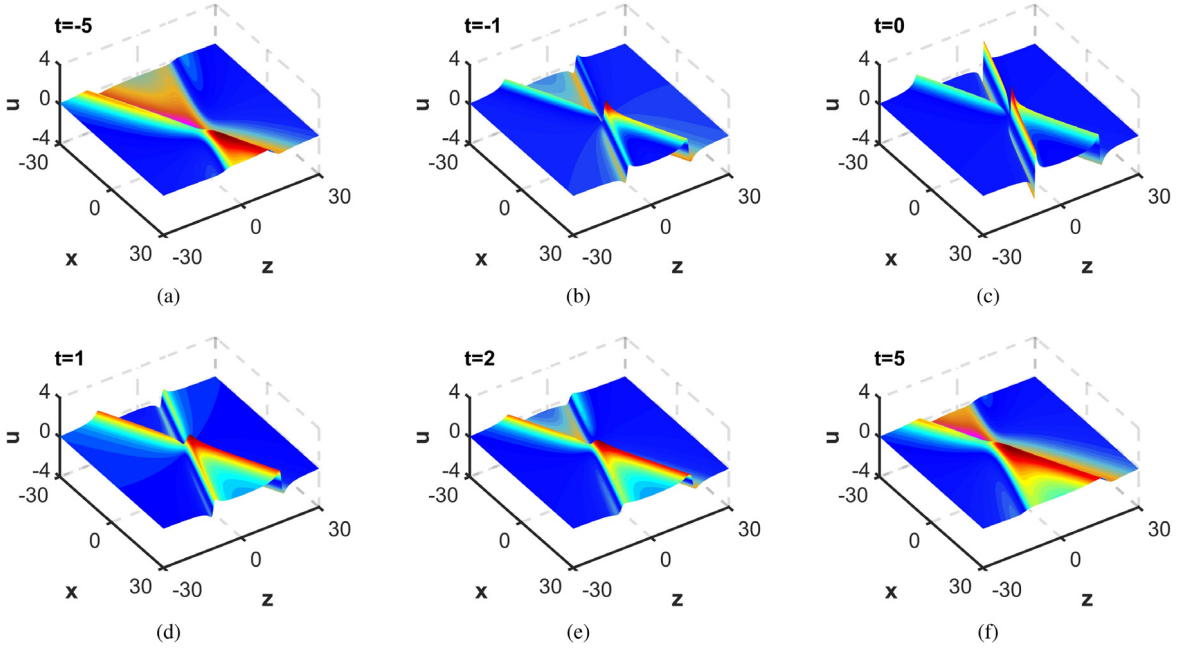


**Fig. 11.** The time evolution of two line rogue waves of Eq. (1) in the $(x, z)$ plane for parameters $a_1 = 1,\ \ b_1 = 2,\ \ a_2 = 1,\ \ b_2 = 2,\ \ c_1 = 3,\ \ c_2 = -2\ d_1 = d_2 = 0$ at $y = 0$.

## 5. The kink soliton interacts with periodic solution, lump and rogue wave

In this section we will construct the interaction solutions of kink soliton with periodic waves, lumps and rogue waves respectively, according to the parameters selection method mentioned above. Next, applying different methods on three soliton, which is at $N = 3$ in Eq. (5), we can derive three types of interaction solutions.

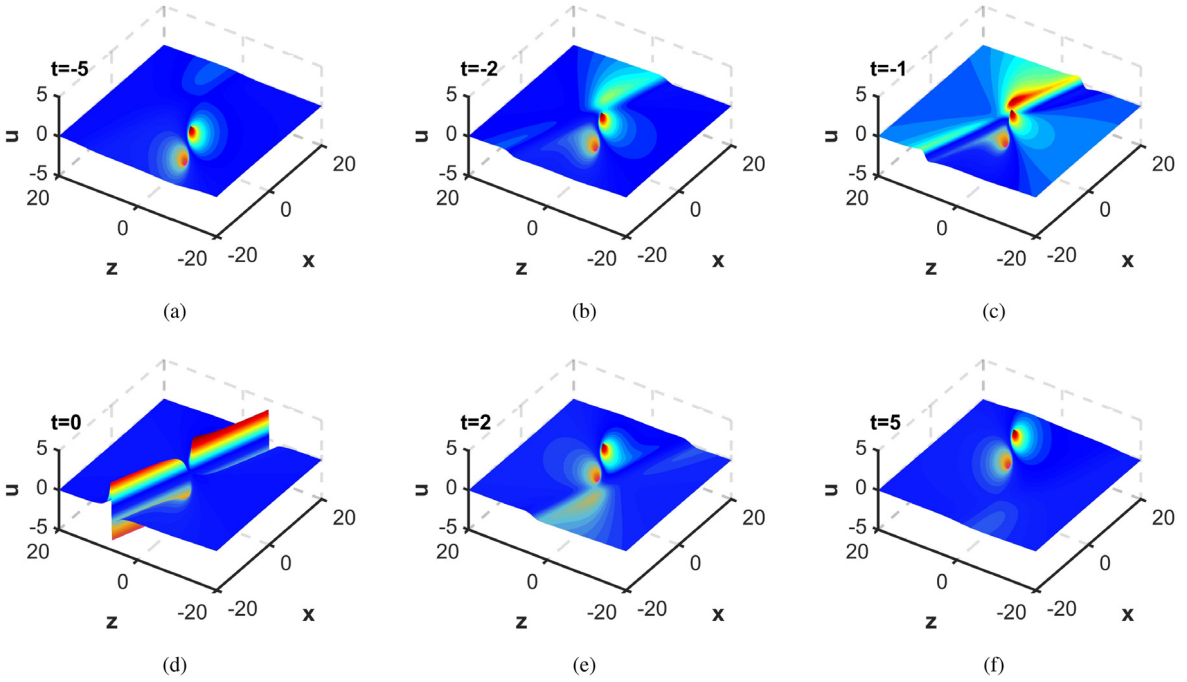


**Fig. 12.** The interaction solution between line rogue wave and lump solution of Eq. (1) in the $(x, z)$ plane for parameters $a_1 = 0.5,\ b_1 = 1,\ a_2 = 0.5,\ b_2 = 1,\ c_1 = -1,\ d_1 = 1\ c_2 = 3\ d_2 = 0$ at $y = 0$.

**Case 1. Interaction between kink soliton and periodic solution**

According to the above method mentioned in Section 3, taking the following parameters $N = 3,\ k_1 = k_3^* = I,\ p_1 = p_3^* = 1 + 3I,\ q_1 = q2 = 2,\ k_2 = 1,\ p_2 = 2,\ q_2 = 1\ , \eta_1^0 = \eta_2^0 = \eta_3^0 = 0$. The interaction solution between periodic solution and soliton can be obtained, which is shown in Fig. 13. Obviously, they have different dynamic behaviors. In the $(x, z)$ plane, the kink soliton interacts with the line breather, while in the other five planes, the kink solitons interact with general breathers.

**Case 2. Interaction between kink soliton and lump**

As the method mentioned in Section 4, applying the long wave limits on the three soliton solutions. And the parameters are set similar to Eq. (12), except for $N = 3$ in Eq. (5), then the corresponding function $f$ is rewritten as

$$f = (\theta_1\theta_2 + a_{12})l_1l_2 + (\theta_1\theta_2 + a_{12} + a_{13}\theta_2 + a_{23}\theta_1 + a_{13}a_{23})l_1l_2e^{\eta_3}, \tag{19}$$

where

$$\begin{aligned} \theta_i &= x + p_iy + q_iz + \frac{q_i^2}{p_i + 1}t, \\ a_{ij} &= -\frac{6(p_i + 1)(p_j + 1)(p_i + p_j)}{((p_i + 1)q_j - q_i(p_j + 1))^2}\ (i < j \le 2), \\ a_{i3} &= -\frac{6(p_i + 1)(p_3 + 1)(p_i + p_3)k_3}{(p_i + 1)(3p_3^2 + p_i + 2p_3)k_3^2 + ((p_i + 1)q_3 - q_i(p_3 + 1))^2}\ (i = 1, 2). \end{aligned} \tag{20}$$

Without loss of generality, setting

$$p_1 = p_2^* = 1 + I,\ \ q_1 = q_2^* = 1 + 3I,\ \ p_3 = 2,\ \ q_3 = 0.5,\ \ \eta_{03} = 0,\ \ k_3 = 1, \tag{21}$$

lump solution can be obtained. whose dynamic behaviors are demonstrated in Fig. 14. It is clear that they have different amplitudes in different planes, but the peaks and valleys of lump solutions are all divided by kink solitons, the peak is located in the high amplitude part of the soliton surface, the valley is located in the low amplitude part of the soliton surface.

**Case 3. Interaction between kink soliton and rogue wave**

In this case, we take the limitation on the three soliton and set $p_1 = p_2*$, all the remaining parameters are real (i.e., $q_1, q_2, q_3, p_3, \eta_{03}, k_3$ are all real), the interaction solution between kink soliton and rogue waves can be obtained. So, without loss of generality, assuming

$$p_1 = p_2^* = 1 + I,\ \ q_1 = q_2 = 2,\ \ p_3 = q_3 = -0.5,\ \ \eta_{03} = 0,\ \ k_3 = 1. \tag{22}$$

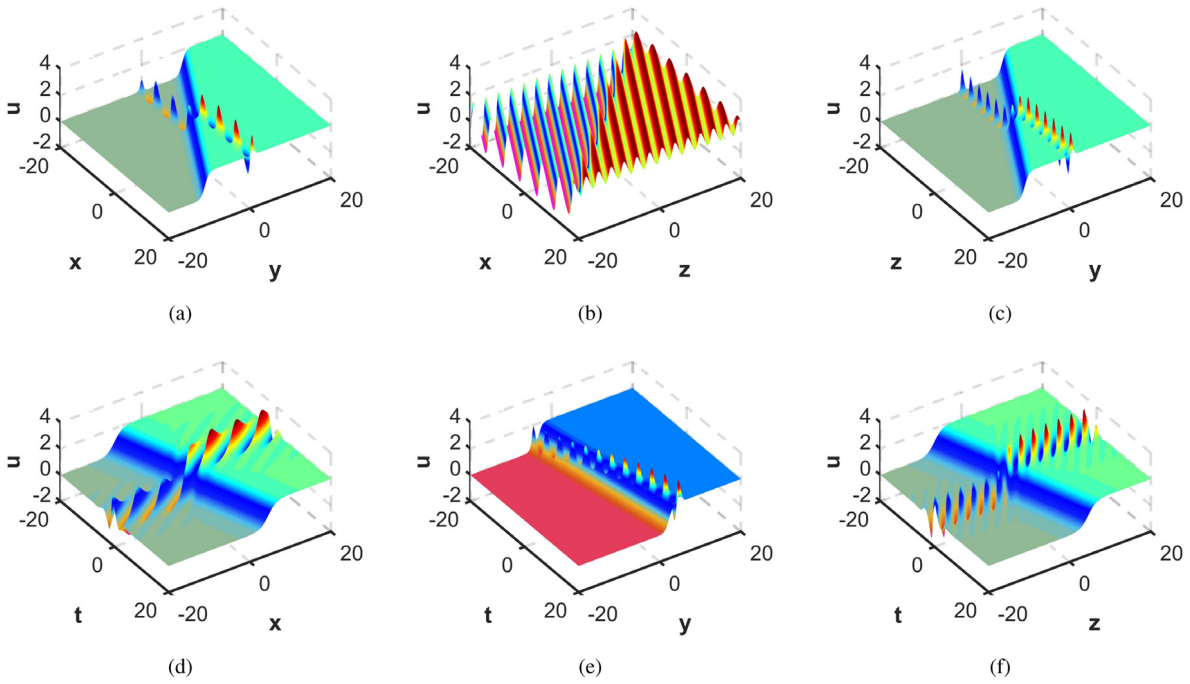


**Fig. 13.** The interaction solution between kink soliton and periodic solution of Eq. (1) in different planes.

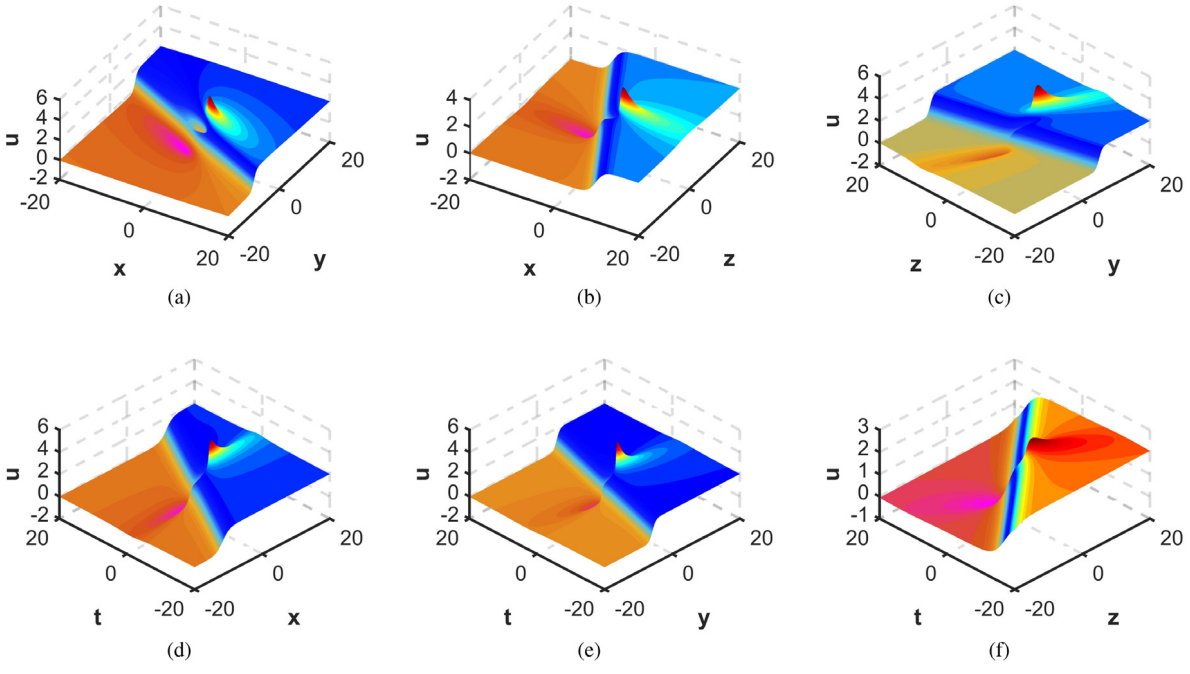


**Fig. 14.** The interaction solution between kink soliton and lump solution of Eq. (1) in the different planes for the same parameters given in Eq. (21).

The dynamic behavior of interaction solution is displayed in Fig. 15. As time goes on, the line rogue wave arises from the constant background and disappears into the constant background again, at the same time, the soliton propagates from left to right. The amplitude of interaction solution reaches a highest value 2.8086 at $t = 0$ in the $(x, z)$ plane.

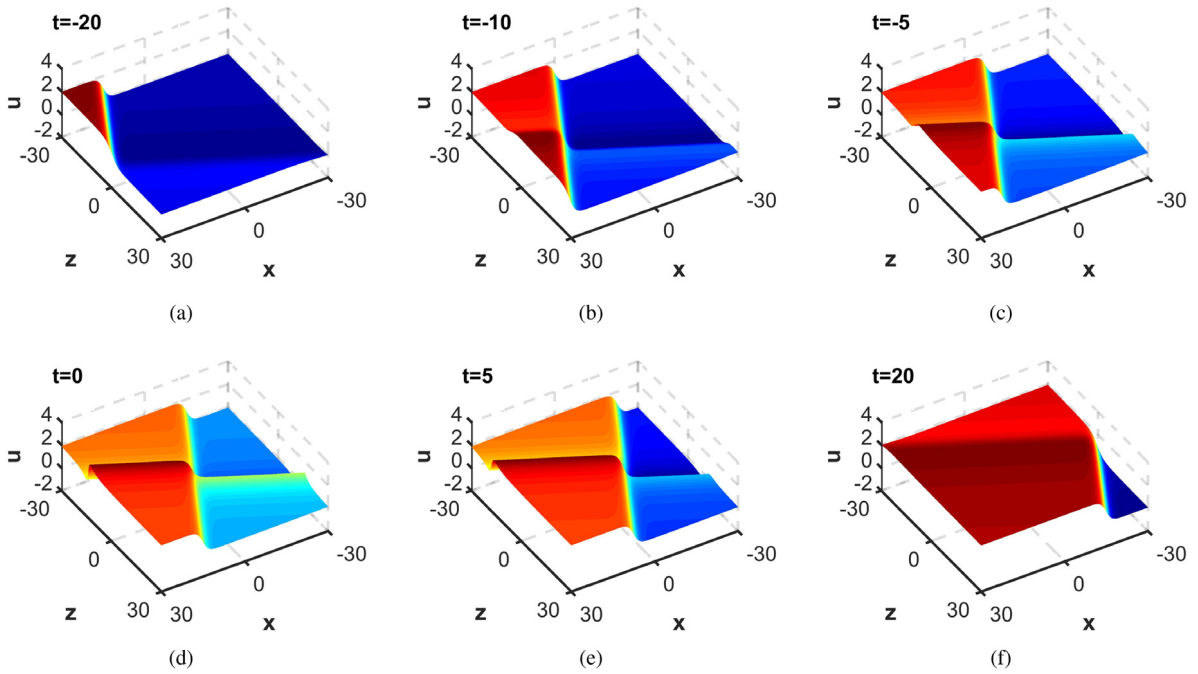


**Fig. 15.** The interaction solution between line rogue waves and kink soliton of Eq. (1) in the $(x, z)$ plane for parameters given in Eq. (22) at $y = 0$.

## 6. Summary and discussions

In summary, localized wave solutions and interaction solutions of the GKP equation have been investigated. According to the bilinear method, $N$ soliton solution of GKP equation is deduced. By virtue of appropriate selections of parameters, line breathers, general breathers and two-order breathers are constructed, respectively. The graphs of their evolution processes over time are presented and their dynamic characteristics are analyzed. Applying the long wave limit method of the soliton solutions, different orders of lumps, rogue waves are constructed, the interaction solutions of these two types solutions are also presented under special parameter constraints. By the same method, interaction solutions between kink solitons and periodic solutions, lump solutions, line rogue waves, are obtained, respectively. They have a variety of different dynamic characteristics. The impacts of the parameters on these solutions are analyzed. The propagation directions, phase shifts, energies and shapes for these solutions can be affected and controlled by the parameters. By taking complex conjugate of the parameters and long wave limit on the soliton solutions, we can obtain different types of localized waves and interaction solutions. The main results can be summarized in the following table:

| $N$-soliton | Method | | | | | |
|---|---|---|---|---|---|---|
| | Complex conjugate | | | Long wave limit | | |
| 2-soliton | LB | GB | | L | LRW | |
| 3-soliton | S + LB | S + GB | | S + L | S + LRW | |
| 4-soliton | Two-LB | Two-GB | LB + GB | Two-LRW | Two-L | L + LRW |

**Note**: S = Soliton, L = Lump, LB = Line breather, GB = General breather, LRW = Line rogues wave.

Moreover, the methods applied in this paper may provide an effective and direct tool to investigate localized waves and interaction solutions of the nonlinear integrable systems. It is worthy of further exploration to apply numerical simulation method to the above theoretical solutions in the future.

## Acknowledgments

We would like to express our sincere thanks to every member in our discussion group for their valuable comments. The project is supported by the Global Change Research Program of China (No. 2015CB9539040), National Natural Science Foundation of China (Nos. 11675054 and 11435005), Outstanding doctoral dissertation cultivation plan of action (No. YB2016039), and Shanghai Collaborative Innovation Center of Trustworthy Software for Internet of Things (No. ZF1213).

## References


[1] C.S. Gardner, J.M. Greene, M.D. Kruskal, R.M. Miura, Method for solving the Korteweg–de Vries equation, Phys. Rev. Lett. 19 (1967) 1095–1097.
[2] M.J. Ablowitz, D.J. Kaup, A.C. Newell, H. Segur, The inverse scattering transform-fourier analysis for nonlinear problems, Stud. Appl. Math. 53 (1974) 249–315.
[3] Y.L. Dang, H.J. Li, J. Lin, Soliton solutions in nonlocal nonlinear coupler, Nonlinear Dynam. 88 (2017) 489–501.
[4] K. Imai, Dromion and lump solutions of the Ishimori-I equation, Progr. Theoret. Phys. 98 (1997) 1013–1023.
[5] D.J. Kaup, The lump solutions and the Bäcklund transformation for the three-dimensional three-wave resonant interaction, J. Math. Phys. 22 (1981) 1176–1181.
[6] W.X. Ma, Lump solutions to the Kadomtsev–Petviashvili equation, Phys. Lett. A 379 (2015) 1975–1978.
[7] J.Y. Yang, W.X. Ma, Abundant lump-type solutions of the Jimbo–Miwa equation in (3+1)-dimensions, Comput. Math. Appl. 73 (2017) 220–225.
[8] H.Q. Zhao, W.X. Ma, Mixed lump-kink solutions to the KP equation, Comput. Math. Appl. 74 (2017) 1399–1405.
[9] J.B. Zhang, W.X. Ma, Mixed lump-kink solutions to the BKP equation, Comput. Math. Appl. 74 (2017) 591–596.
[10] J.Y. Yang, W.X. Ma, Z.Y. Qin, Lump and lump-soliton solutions to the (2+1)-dimensional Ito equation, Anal. Math. Phys. (2017). http://dx.doi.org/10.1007/s13324-017-0181-9.
[11] W.X. Ma, X.L. Yong, H.Q. Zhang, Diversity of interaction solutions to the (2+1)-dimensional Ito equation, Comput. Math. Appl. 75 (2018) 289–295.
[12] W.X. Ma, Y. Zhou, Lump solutions to nonlinear partial differential equations via Hirota bilinear forms, J. Differential Equations 264 (2018) 2633–2659.
[13] D.J. Kedziora, A. Ankiewicz, N. Akhmediev, Second-order nonlinear Schrödinger equation breather solutions in the degenerate and rogue wave limits, Phys. Rev. E 85 (2012) 066601.
[14] M. Tajiri, T. Arai, Growing-and-decaying mode solution to the Davey–Stewartson equation, Phys. Rev. E 60 (1999) 2297.
[15] N. Akhmediev, J.M. Soto-Crespo, A. Ankiewicz, How to excite a rogue wave, Phys. Rev. A 80 (2009) 043818.
[16] C. Liu, Z.Y. Yang, L.C. Zhao, W.L. Yang, Vector breathers and the inelastic interaction in a three-mode nonlinear optical fiber, Phys. Rev. A 89 (2014) 055803.
[17] J.S. He, H.R. Zhang, L.H. Wang, A.S. Fokas, Generating mechanism for higher-order rogue waves, Phys. Rev. E 87 (2013) 052914.
[18] N. Akhmediev, V.I. Korneev, Modulation instability and periodic solutions of the nonlinear Schrödinger equation, Theoret. Math. Phys. 69 (1986) 1089–1093.
[19] Y.C. Ma, On the multi-soliton solutions of some nonlinear evolution equations, Stud. Appl. Math. 60 (1979) 73–82.
[20] A. Chabchoub, N.P. Hoffmann, N. Akhmediev, Rogue wave observation in a water wave tank, Phys. Rev. Lett. 106 (2011) 204502.
[21] Y. Ohta, J.K. Yang, Rogue waves in the Davey–Stewartson I equation, Phys. Rev. E 86 (2012) 036604.
[22] B.L. Guo, L.M. Ling, Q.P. Liu, Nonlinear Schrödinger equation: Generalized Darboux transformation and rogue wave solutions, Phys. Rev. E 85 (2012) 026607.
[23] Z.Y. Yan, Vector financial rogue waves, Phys. Lett. A 375 (2011) 4274–4279.
[24] S.H. Chen, L.Y. Song, Rogue waves in coupled Hirota systems, Phys. Rev. E 87 (2013) 032910.
[25] G. Mu, Z.Y. Qin, R. Grimshaw, Dynamics of rogue waves on a multisoliton background in a vector nonlinear Schrodinger equation, J. Appl. Math. 75 (2015) 1–20.
[26] C.Q. Dai, X.G. Wang, J.F. Zhang, Nonautonomous spatiotemporal localized structures in the inhomogeneous optical fibers: Interaction and control, Ann. Phys. 326 (2011) 645–656.
[27] L.M. Ling, L.C. Zhao, Simple determinent representation for rogue waves of the nonlinear schrödinger equation, Phys. Rev. E 88 (2013) 043201.
[28] X. Wang, Y.Q. Li, F. Huang, Y. Chen, Rogue wave solutions of AB system, Commun. Nonlinear Sci. Numer. Simul. 20 (2015) 434–442.
[29] J.C. Chen, Y. Chen, B.F. Feng, K.-i. Maruno, Rational solutions to two- and one-dimensional multicomponent Yajima-Oikawa systems, Phys. Lett. A 379 (2015) 1510–1519.
[30] Y.F. Yue, L.L. Huang, Y. Chen, N-solitons, breathers, lumps and rogue wave solutions to a (3+1)-dimensional nonlinear evolution equation, Comput. Math. Appl. 75 (2018) 2538–2548.
[31] L. Draper, Freak wave, Mar. Obs. 35 (1965) 193–195.
[32] D.A.G. Walker, P.H. Taylor, R.E. Taylor, The shape of large surface waves on the open sea and the Draupner new year wave, Appl. Ocean Res. 26 (2005) 73–83.
[33] D.R. Solli, C. Ropers, P. Koonath, B. Jalali, Optical rogue waves, Nature 450 (2007) 1054.
[34] B. Kibler, J. Fatome, C. Finot, G. Millot, F. Dias, The peregrine soliton in nonlinear fibre optics, Nat. Phys. 6 (2010) 790–795.
[35] W.X. Ma, E.G. Fan, Linear superposition principle applying to Hirota bilinear equations, Comput. Math. Appl. 61 (2011) 950–959.
[36] F.C. You, T.C. Xia, D.Y. Chen, Decomposition of the generalized KP, cKP and mKP and their exact solutions, Phys. Lett. A 372 (2008) 3184–3194.
[37] B.B. Kadomtsev, V.I. Petviashvili, On the stability of solitary waves in weakly dispersing media, Sov. Phys. Dokl. 15 (1970) 539–541.
[38] A.M. Wazwaz, S.A. El-Tantawy, A new (3+1)-dimensional generalized Kadomtsev–Petviashvili equation, Nonlinear Dynam. 84 (2016) 1107–1112.
[39] W.X. Ma, A. Abdeljabbar, M.G. Asaad, Wronskian and Grammian solutions to a (3+1)-dimensional generalized KP equation, Appl. Math. Comput. 217 (2011) 10016–10023.
[40] W.X. Ma, Z.N. Zhu, Solving the (3+1)-dimensional generalized KP and BKP equations by the multiple exp-function algorithm, Appl. Math. Comput. 218 (2012) 11871–11879.
[41] W.X. Ma, A. Abdeljabbar, A bilinear Bäcklund transformation of a (3+1)-dimensional generalized KP equation, Appl. Math. Lett. 25 (2012) 1500–1504.
[42] W.X. Ma, T.C. Xia, Pfaffianized systems for a generalized Kadomtsev–Petviashvili equation, Phys. Scr. 87 (2013) 055003.
[43] W.X. Ma, Z.Y. Qin, X. Lü, Lump solutions to dimensionally reduced p-gKP and p-gBKP equations, Nonlinear Dynam. 84 (2016) 923–931.
[44] A. Abdeljabbar, W.X. Ma, A. Yildirim, Determinant solutions to a (3+1)-dimensional generalized KP equation with variable coefficients, Chinese Ann. Math. 33B (2012) 641–650.
[45] A.M. Wazwaz, Multiple-soliton solutions for a (3+1)-dimensional generalized KP equation, Commun. Nonlinear Sci. Numer. Simul. 17 (2012) 491–495.
[46] J.P. Wu, X.G. Geng, Novel Wronskian condition and new exact solutions to a (3+1)-dimensional generalized KP equation, Commun. Theor. Phys. 60 (2013) 556–560.
[47] Y.N. Tang, W.J. Zai, New exact periodic solitary-wave solutions for the (3+1)-dimensional generalized KP and BKP equations, Comput. Math. Appl. 70 (2015) 2432–2441.
[48] H.L. Chen, Z.H. Xu, Z.D. Dai, Kink degeneracy and rogue potential flow for the (3+1)-dimensional generalized Kadomtsev–Petviashvili equation, Therm. Sci. 20 (2016) S919–S927.
[49] L. Cheng, Y. Zhang, Wronskian and linear superposition solutions to generalized KP and BKP equations, Nonlinear Dynam. 90 (2017) 355–362.
[50] J.G. Liu, Y. Tian, Z.F. Zeng, New exact periodic solitary-wave solutions for the new (3+1)-dimensional generalized Kadomtsev–Petviashvili equation in multi-temperature electron plasmas, AIP Adv. 7 (2017) 105013.
[51] S.T. Mohyud-Din, A. Irshad, N. Ahmed, U. Khan, Exact solutions of (3+1)-dimensional generalized KP equation arising in physics, Results Phys. 7 (2017) 3901–3909.

[52] X.B. Wang, S.F. Tian, H. Yan, T.T. Zhang, On the solitary waves, breather waves and rogue waves to a generalized (3+1)-dimensional Kadomtsev–Petviashvili equation, Comput. Math. Appl. 74 (2017) 556–563.
[53] J.G. Rao, Y. Cheng, J.S. He, Rational and semirational solutions of the nonlocal Davey–Stewartson equations, Stud. Appl. Math. 139 (2017) 568–598.
[54] C. Qian, J.G. Rao, Y.B. Liu, J.S. He, Rogue waves in the three-dimensional Kadomtsev–Petviashvili equation, Chin. Phys. Lett. 33 (2016) 110201.
[55] R. Hirota, The Direct Method in Soliton Theory, Cambridge University Press, 2004.
[56] M.J. Ablowitz, J. Satsuma, Solitons and rational solutions of nonlinear evolution equations, J. Math. Phys. 19 (1979) 2180–2186.
[57] J. Satsuma, M.J. Ablowitz, Two-dimensional lumps in nonlinear dispersive systems, J. Math. Phys. 20 (1979) 1496–1503.